Nitric Oxide 90 (2019) 29–36

Contents lists available at ScienceDirect

Nitric Oxide

journal homepage: www.elsevier.com/locate/yniox

New generation of nitric oxide-releasing porous materials: Assessment of their potential to regulate biological functions

Rosana V. Pinto[a,b], Ana C. Fernandes[b], Fernando Antunes[b], Zhi Lin[c], João Rocha[c], João Pires[b], Moisés L. Pinto[a,*]

[a] CERENA, Department of Chemical Engineering, Instituto Superior Técnico, University of Lisbon, 1049-001, Lisbon, Portugal
[b] CQB and CQE, Department of Chemistry and Biochemistry, Faculty of Sciences, University of Lisbon, Ed. C8, Campo Grande, 1749-016, Lisbon, Portugal
[c] CICECO - Aveiro Institute of Materials, Department of Chemistry, University of Aveiro, Campus Universitário de Santiago, 3810-193, Aveiro, Portugal

ARTICLE INFO

Keywords:
Adsorption
Nitric oxide
NO donors
Controlled delivery systems
Porous materials
Wound healing

ABSTRACT

Nitric oxide (NO) presents innumerable biological roles, and its exogenous supplementation for therapeutic purposes has become a necessity. Some nanoporous materials proved to be potential vehicles for NO with high storage capacity. However, there is still a lack of information about their efficiency to release controlled NO and if they are biocompatible and biologically stable. In this work, we address this knowledge gap starting by evaluating the NO release and stability under biological conditions and their toxicity with primary keratinocyte cells. Titanosilicates (ETS-4 and ETS-10 types) and clay-based materials were the materials under study, which have shown in previous studies suitable NO gas adsorption/release rates.

ETS-4 proved to be the most promising material, combining good biocompatibility at 180 μg/mL, stability and slower NO release. ETS-10 and ETAS-10 showed the best biocompatibility at the same concentration and, in the case of clay-based materials, CoOS is the least toxic of those tested and the one that releases the highest NO amount. The potentiality of these new NO donors to regulate biological functions was assessed next by controlling the mitochondrial respiration and the cell migration. NO-loaded ETS-4 regulates O_2 consumption and cell migration in a dose-dependent manner. For cell migration, a biphasic effect was observed in a narrow range of ETS-4 concentration, with a stimulatory effect becoming inhibitory just by doubling ETS-4 concentration. For the other materials, no effective regulation was achieved, which highlights the relevance of the new assessment presented in this work for nanoporous NO carriers that will pave the way for further developments.

1. Introduction

The potential outcome of the controlled delivery of nitric oxide (NO) to specific biological targets led to the development of new NO-carrying and releasing matrices for therapeutic benefit. Among its many biological roles, NO is a strong vasodilator, antimicrobial agent and wound healing accelerator, and its use as a therapeutic agent provides an excellent alternative to conventional drugs [1,2]. Generically, therapy relies both on NO donors that release the molecule in a direct or indirect way (*i.e.*, via metabolic activity, biotransformation or redox activation), and on agents that increase NO bioactivity [3]. Most of existing molecular donors present, however, certain limitations when in contact with biological fluids, namely high solubility, non-target and uncontrolled NO release and the release of toxic decomposition products (*e.g.* carcinogenic nitrosamines) [4–6]. For example, due to its high solubility, NO may be released before reaching the target site, thus requiring higher amounts of donor to meet the therapeutic needs, triggering potential toxic effects [4]. Under these circumstances, additional chemical reactions become relevant, generating reactive nitrogen oxide species capable to inhibit cell respiration and to induce cell toxicity [5].

Recent work has unveiled the NO adsorption/release potential of nanoporous framework solids bearing metal active sites [5,6]. These new materials overcome the limitations of the most conventional donors because they provide a safe storage and controlled delivery of pure NO in the target tissue, being of special interest for topical applications [5]. In addition, the amount of NO and the release period may be modulated, by tuning the porosity of the material and/or varying the nature and the number of metal sites in the framework [6–8].

Several types of porous materials have recently been studied for this

* Corresponding author. Departamento de Engenharia Química, Instituto Superior Técnico, Universidade de Lisboa, Av. Rovisco Pais, no 1, 1049-001, Lisboa, Portugal.
E-mail address: moises.pinto@tecnico.ulisboa.pt (M.L. Pinto).

https://doi.org/10.1016/j.niox.2019.05.010
Received 5 February 2019; Received in revised form 22 March 2019; Accepted 28 May 2019
Available online 30 May 2019
1089-8603/

Table 1
Porous materials studied in this work presenting suitable NO gas adsorption and release properties.

MATERIAL	DESCRIPTION	ADSORPTION CAPACITY (%)	RELEASE CAPACITY (% M/M)	REF.
ETS-10	Titanosilicate with hexacoordinated framework Ti^{4+}	8	3	[13]
ETAS-10	ETS-10 with isomorphous substitution of framework Si^{4+} by Al^{3+}	12	5	[13]
ETGS-10	ETS-10 with isomorphous substitution of framework Si^{4+} by Ga^{3+}	16	2.9	[13]
ETS-4	Titanosilicate with unsaturated (pentacoordinated) Ti^{4+}	11	5	[11]
Cu-ETS-4	ETS-4 with extra-framework cations exchanged by Cu^{2+}	12	6.3	[12]
Co-ETS-4	ETS-4 with extra-framework cations exchanged by Co^{2+}	7	4	[12]
SEPIOLITE	Natural clay	1	0.6	[10]
CoOS	Smectite clay with Co^{2+} in the structure using tetramethyl orthosilicate as a silicon source	5.1	2	[15]
CoAS-B	Smectite clay with Co^{2+} in the structure using silicic acid as a silicon source	3.5	1	[15]
L-HM-1	Organoclay with the modification of aluminum silicate (montmorillonite) with L-histidine	3.2	1.4	[16]

purpose, including: zeolites, clays, metal-organic frameworks (MOFs) and titanosilicates [7,9–11]. We have been interested in designing new porous structures for the storage and controlled release of NO. We showed that microporous titanosilicates (ETS-4) containing Ti^{4+} unsaturated metal centres and Cu^{2+} or Co^{2+} extra-framework cations exhibit exceptional properties to adsorb and release controlled NO amounts [11,12].Another microporous titanosilicate structure, ETS-10, and the effect of its isomorphic substitution of Si by Al and Ga, was also explored [13], as well as materials based on modified mineral clays (sepiolite and montmorillonite) [10,14], synthetic clays (smectite clays with cobalt ions) [15] and organoclays (natural clays modified with L-histidine) [16]. Clay-based materials, although storing less NO than titanosilicates and displaying faster NO release still release NO amounts that may trigger positive biological responses.

So far, studies using these new donors concerning their biocompatibility, stability and control of biological processes with the NO released are still poorly explored. Only few papers, using MOFs and zeolites based materials, demonstrated that NO released from those materials is able to inhibit platelet aggregation [7,17], to relax smooth muscle of blood vessels [8] and stimulate the wound healing process [18]. However, no actual demonstration of control of the biological systems was provided, namely by establishing a relationship between the response extension/intensity and the amount of NO released to the system. This is of central importance to modulate the response of the biological systems at the therapeutic level and the present work aims to provide this demonstration and afford a more comprehensive assessment of the real potentialities of the materials.

The work starts by evaluating the biocompatibility using primary keratinocyte cells (HEKn), the materials' stability in biological fluids and following with the evaluation of NO release under biological conditions. Materials that exhibited the best combination of good biocompatibility, stability and NO slower release were then evaluated to control two relevant cellular processes: (1) mitochondrial respiration and (2) cell migration, in two independent assessments. We demonstrate in this work that not all materials that are able to store and release NO can be used in biological systems, since they should combine several characteristics to provide a successful effect.

2. Materials and methods

2.1. Materials

ETS-4 was synthesized with an alkaline solution made by dissolving 33.16 g of meta-silicate (BDH), 2.00 g NaOH (Merck), and 3.00 g KCl (Merck) into 25.40 g H_2O. 31.88 g of $TiCl_3$ (15% m/m, $TiCl_3$ and 10% m/m HCl, Merck) was added to this solution and stirred thoroughly. This gel was transferred to a Teflon-lined autoclave and treated at 230 °C for 17 h. The product was filtered off, washed at room temperature with distilled water and dried at 70 °C overnight, the final product being an off-white microcrystalline powder. This synthesis optimization and product characterization are described elsewhere [19]. Cu and Co exchanged ETS-4 was prepared by cation exchange with $CuNO_3$ and $CoNO_3$ solutions, and the products characterized as previously described [12].

ETS-10, ETAS-10 and ETGS-10 were synthesized according to previously optimized procedures described elsewhere [20–22], using titanium trichloride as Ti source. The materials were characterized as previously described to ascertain their purity and porosity [13].

Sepiolite-type natural clay was obtained from the Tolsa Group, Spain. Organoclay modified with L-histidine and modified synthetic clays were synthetized according to the procedures previously described by Fernandes et al. [15,16].

To confirm the synthesis' purity and the solid phases obtained the materials were characterized by powder X-ray diffraction (XRD) and nitrogen adsorption at −196 °C. The detailed description of those experimental methods and the obtained results are in Section I of the Supplementary material. All the obtained data are coincident with the literature, which ensures the purity of the newly synthesized materials [10–13,15,16,19–22]. Moreover, a brief description of the materials used in this study and their NO adsorption/release capacities are shown in Table 1. These materials represent a selection from the studied materials by our group to date that present the most promising NO storage and release properties.

2.2. NO adsorption and storage in the materials

Loading of the material with NO was proceeded by introducing each sample in a glass vacuum cell with a valve and degassed under high-vacuum conditions (better than 10^{-2} Pa) to activate the samples. Time and heating temperatures for degassing were different depending on the material: For ETS-4 and modified specimens, the conditions used were 100 °C for 3 h [12]; ETS-10, ETAS-10 and ETGS-10 were heated at 300 °C for 2.5 h [13]; Sepiolite was heated at 250 °C for 2 h [10]; Modified organoclay with L-histidine (L-HM-1) was degassed at 150 °C for 2.5 h [16] and modified synthetic clays (CoOS and CoAS-B) at 250 °C for 2.5 h [15]. After outgassing and with the material already at room temperature, NO was admitted to the vacuum cell housing the solid, at a pressure of 80 kPa, and kept there for 3 days. After this period of NO loading, the remaining gas was evacuated by connecting the cell to the vacuum line and opening the valve. The loaded material was stored by filling immediately the valve with helium up to atmospheric pressure.

2.3. NO release profiles in biological media

NO released over time by the materials was quantified in biological medium (RPMI-1640 with 10% (*V/V*) fetal bovine serum, penicillin-streptomycin (100 UI/mL and 100 µg/mL, respectively) using the method of Griess at 37 °C. This is an indirect method, which quantify its decomposition product (NO_2^-) accumulated in the medium over time [23]. After 15, 30, 60 and 120 min, 2 mL of sample with a material concentration of 450 µg/mL was centrifuged in order to separate the

material from the medium. Other concentrations were tested for ETS-4 (180, 90 and 45 μg/mL). Subsequently, the supernatant obtained after centrifugation was incubated with Griess reagent (0.2% naphthylethylenediamine dihydrochloride, and 2% sulphanilamide in 5% phosphoric acid) generating a chromophoric azo product, which was quantified by absorbance at 548 nm, using a microplate reader (Tecan, A-5082 Sunrise Remote). A calibration curve was prepared using a sodium nitrite solution (0–200 μM) according to the same procedure described above for the samples.

2.4. Material's stability in biological medium

The material's stability in complete cellular culture medium (EpiLife® - same used for HEKn cells culture) was evaluated under cell incubation conditions (37 °C, humidified atmosphere with 5% CO_2) after 72 h (maximum time of the accomplished cellular assays), using a material concentration of 450 μg/mL. Depending on the material's structure, the determination of the correspondent metal(s) content in the medium was done by ICP at the laboratory of analysis of Instituto Superior Técnico, following the analytical procedure defined in the standard ISO 11885:2007.

Powder X-ray diffraction was performed using a Philips X-ray diffractometer (PW 1730) with automatic data acquisition (APD Philips v3.6B), using Cu Kα radiation (λ = 0.15406 nm). The diffraction patterns were collected in the 2θ range of 5°–20° with a 0.01° step size and an acquisition time of 200 s per step.

2.5. HeLa and HEKn cells culture

HeLa cells (human cervical cancer cell line) (American Type Culture Collection, Manassas, VA, USA) were cultured in supplemented RPMI-1640 with fetal bovine serum (10% *V/V*), penicillin-streptomycin (100 UI/mL and 100 μg/mL, respectively) and 2 mM glutamine, and incubated at normal culturing conditions (37 °C, 5% CO_2). Fresh medium was replaced every 2 days up to adequate confluency for subcultivation.

HEKn cells (epidermal keratinocytes isolated from neonatal foreskin) (Thermo Fisher Scientific) were cultivated in EpiLife® Medium supplemented with 60 μM calcium, an antibiotic/antimycotic solution of gentamicin and amphotericin B and an human keratinocyte growth supplement (1% V/V; composed by bovine pituitary extract (0.2% V/V), recombinant human insulin-like growth factor-I (1 μg/mL), hydrocortisone (0.18 μg/mL), bovine transferrin (5 μg/mL) and human epidermal growth factor (0.2 ng/mL)) and an antibiotic/antimycotic solution of gentamicin and amphotericin B, incubated and maintained in the conditions of HeLa cells.

2.5.1. HEKn cytotoxicity tests

Viability/toxicity was assessed by the fluorometric alamarBlue® assay. HEKn cells were seeded in 96-well plates at a density of 7500 or 5000 cells per well for the 24 or 72 h experiments, respectively. After 24 h of incubation, the media were replaced by the supplemented medium containing the desired concentration of the compound. Two concentrations were tested: 450 μg/mL and 180 μg/mL. Eight replicates were used for each condition.

On the respective time, 10 μL of alamarBlue® was added directly to each well and the plate was incubated for at least 4 h alamarBlue® reduction was quantified by fluorescence (λ_{ex} = 530 nm, λ_{em} = 590 nm) in a Spectra Max Gemini EM reader from Molecular Devices. Cell viability was calculated as follows:

$$cell\ viability(\%) = \frac{F_{(cells+material)}}{F_{control\ (cells)}} \times 100$$

Where $F_{(cells+material)}$ represents the average of the fluorescence obtained for the cells incubated with the material and $F_{control(cells)}$ the fluorescence average of the control, which corresponds to the cells incubated only with the medium. The fluorescence signal of the supplemented medium was subtracted in all the conditions.

2.5.2. Measurement of oxygen consumption rates using HeLa cells

Mitochondrial respiration was measured at 37 °C using an oxygen electrode. HeLa cells (2.5 mg of protein) were resuspended in 40 μL PBS, kept in ice for 5 min and incubated in the O_2 electrode chamber containing a specific respiration buffer (0.07 M sucrose, 0.23 M mannitol, 30 mM Tris HCl, 4 mM $MgCl_2$, 5 mM KH_2PO_4, 1 mM EDTA and 0.5% bovine serum albumin, pH 7.4) and with 0.01% digitonin (to permeabilize the cells) under stirring. Respiratory substrate (20 mM succinate) was added to the mitochondrial incubation (state 4). State 3 active respiration was obtained by adding ADP (0.125 mM), allowing the ATP synthase to function, proton motive force to drop and election transport to accelerate. Finally, the NO-loaded material was added at the desired concentration. The following concentrations were tested: 450, 180 and 90 μg/mL. Respiration rates (O_2 consumption) were calculated as the negative time derivative of oxygen concentration using the Oxygraph plus program. Considering the maximum respiration rate reached in state 3, the mitochondrial inhibition by the NO is expressed comparatively to that value. Since O_2 consumption showed some variation from day to day, the respiration rate is reported as percentage of control.

Preliminary studies were performed without cells, by adding the different tested concentrations of NO-loaded material, confirming no interference with the signal. Moreover, unloaded material was also tested and no significant inhibition of the mitochondrial respiration was observed.

2.5.3. Cell migration assay

For this process, the Oris™ Cell Migration Assay (Platypus technologies, LLC, Madison WI) was used by adapting the manufacturer's protocol and using HeLa cells with a confluent density of 5×10^4 per well NO-loaded material was tested using different concentrations and, in parallel, the unloaded material was also tested, as control. Cells were allowed to migrate into the central detection zone for 48 h. Images were captured at pre-migration time (0 h) and after 6, 12, 24 and 48 h using a microscope (Olympus, CK40) equipped with a digital camera (C4040; Olympus). For that, a black mask with 96 prefabricated openings that precisely frame the central detection zone of each well, was attached to the bottom of the 96-well plate. The quantification of cell migration was performed by imaging analysis using ImageJ 1.50i software. All images covered the entire detection zone and the surrounding area was black due to the masking plate. Using a MRI wound healing tool [24], it was possible to adjust a threshold in order to obtain the value of the free area inside the detection zone that was not occupied by cells. The migrated cells area at each time was calculated using equation (1):

% cell migration or wound closur

$$e = \frac{(Area_{pre-migration\ (t=0\ h)} - Area_{post-migration\ (t=x\ h)}}{Area_{pre-migration\ (t=0\ h)}} \cdot 100 \quad (1)$$

The average percentage of wound closure and standard deviation of the three independent assays with four replicates each were reported in the results. Since, some variability is always present between independent assays, the results are reported as the difference in closure percentage between the control (only cells) and the cells with the new donor. Statistical analysis was performed using unpaired student's t-test and the level of statistical difference was defined at $p < 0.05$.

3. Results

3.1. HEKn biocompatibility

Biocompatibility is a key for understanding the host response to a material [25]. In this context, preliminary cytotoxic tests with HeLa

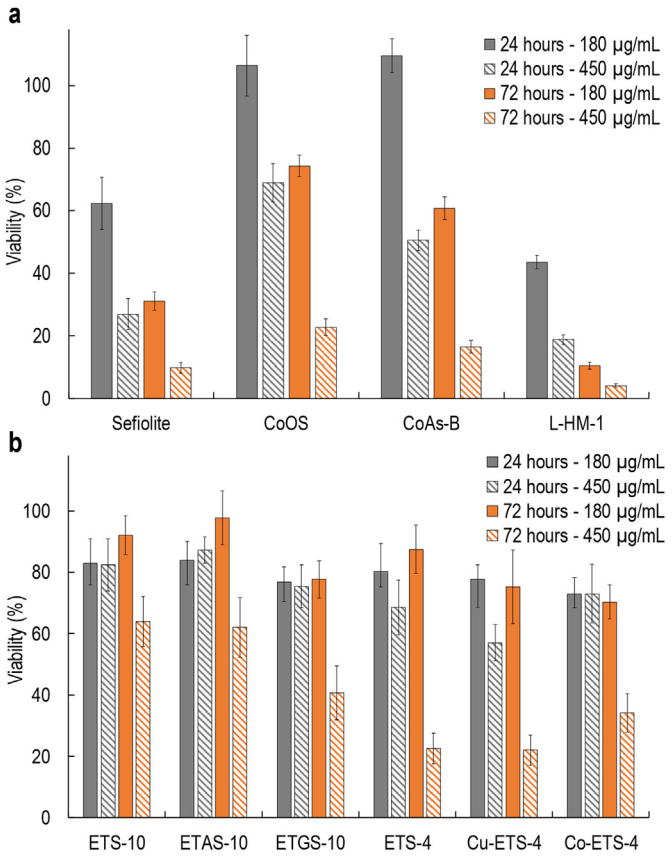

Fig. 1. Cytotoxicity assays with selected porous materials.
Viability results for **a)** clay-based materials and **b)** selected titanosilicates using primary keratinocytes (HEKn) after 24 and 72 h of incubation. All materials were tested without NO, at a concentration of 450 and 180 µg/mL, represented by striped and solid bars, respectively. The error bars represent the standard deviation of eight replicates.

cells have already been performed for titanosilicates [12,13] and clays [10,15,16], showing very encouraging results. In order to better evaluate toxicity, here we report additional tests with primary human cells. HEKn cells were chosen due to the potential application of these materials in wound healing treatments. The obtained results are shown in Fig. 1 a and b for clay-based and titanosilicate-based porous materials, respectively. Since our objective was to compare the materials and not to establish the toxicity threshold, two concentrations were tested, 180 and 450 µg/mL, the latter being at the upper limit usually used for evaluating the cytotoxicity of silicas and other porous materials [26,27] (this concentration was also used in the previous HeLa tests).

For clay-based samples (Fig. 1 a), results with the higher concentration (450 µg/mL) reflected high toxicity after 72 h, with 20% cells survival at best case (CoOS). At low concentration (180 µg/mL) CoOS and CoAs–B present no toxicity after 24 h and a survival rate of at least 60% after 72 h. Since the natural clay sepiolite and L-HM-1 present toxicities higher than 50% after 72 h even at low concentration, their use in biological systems is not recommended.

The biocompatibility results of titanosilicates (Fig. 1 b) revealed a considerable toxicity at the longer exposure time (72 h) at high concentration (striped bars), which is more evident in ETS-4 and ETS-4 based materials (toxicity > 70%). At low concentrations (full bars), cells' survival increased significantly (75% viability for the worst case, Co-ETS-4). Additionally, toxicity was assessed with selected materials loaded with NO and compared with unloaded ones (Supplementary Figure A8). Although high amounts of material have been used (450 µg/mL) in both conditions, no significant differences in toxicity were observed, which indicates that the concentration of NO released by these materials (450 µg/mL) is not enough to induce toxicity.

Overall, results demonstrated an increased susceptibility when using primary cells, comparing with the results obtained with HeLa cells [10,12,13,15,16]. For instance, HeLa cells in contact with sepiolite at 450 µg/mL presented ~70% cell survival after 72 h [10], in clear contrast with the ~10% cell survival observed with HEKn cells in the present work (Fig. 1). Comparing with other porous materials studied for this purpose, for instance vitamin B_3 MOFs with Ni and Co metal centres [9], both MOFs present toxicities higher than 60% at 450 µg/mL after 72 h in contact with the same cell line. This toxicity is comparable with the results presented here (Figs. 1 and 2) for most of the materials. Tests of common zeolites carried out with various cell lines [18,28–30] show that those materials are less toxic (20% at high concentration) than most materials assessed in this work. However, zeolites present lower NO adsorption/release capacity.

3.2. NO release and materials' stability in biological media

Having knowledge about the NO release behaviour of these materials under biological environments is also extremely important for developing useful therapeutics, since beneficial effects of any NO-based drug depend strongly on the concentration and duration of the NO delivery [31]. Previous studies of NO release kinetics in liquid phase relied on the oxyhemoglobin assay [32], using a haemoglobin solution at room temperature [11]. However, for a more consistent evaluation, the physiological medium used should mimic closely that of the proposed application. For example, the amount of available NO released

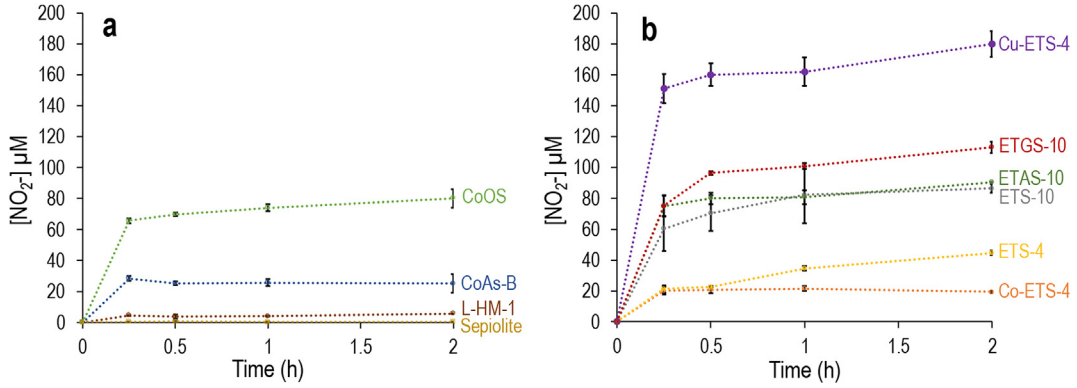

Fig. 2. Nitric oxide release studies under biological conditions.
Concentration of nitrite measured by Griess reagent assay in supplemented RPMI-1640 medium in the presence of NO-loaded materials at a concentration of 450 µg/mL: a) release profiles from the selected modified clays and b) release profiles from the selected modified titanosilicates. All the measurements were performed at 37 °C. The error bars represent the standard deviation of three assays.

from a material in blood is significantly lower than in phosphate buffered saline solution [33]. Thus, NO release studies were performed in the present work using the Griess reagent assay under *in vitro* biological conditions. Fig. 2a) and b) displays the NO release profiles obtained for titanosilicates and clays, respectively.

On the overall, titanosilicates release higher amounts of NO than clays, with exception to the CoOS which presented a release within the range of the titanosilicates. In three specific cases, ETS-4, ETGS-10 and Cu-ETS-4, the release can be controlled over time as shown by the slow increase of nitrite in the solution, particularly in the ETS-4 case. For this material, the NO released amount increased almost linearly with time, which is the most favourable release kinetic for drug delivery systems [34]. Although ETS-4 was not the material that releases the highest amount of NO, it ensures that no exaggerated amounts of NO are released in the first few minutes, since this effect may induce toxicological effects on the surrounding tissues. The highest nitrite release at 450 μg/mL was achieved by Cu-ETS-4 (up to 180 μM), with the highest amount of NO being released in the first few minutes. Similarly, a fast (up to 15 min) NO release is observed from ETS-10 and related materials (ETAS-10 and ETGS-10), which may be limiting for future therapeutic applications.

Regarding clay-based materials, L-HM-1 and Sepiolite do not release any significant amounts of NO, whereas CoOS is the most promising material (80 μM nitrite after 2 h), but this release is very fast which may limit its applicability.

Overall, titanosilicates clearly released higher amounts, as was previously demonstrated through NO adsorption/desorption studies of each material (Table 1). Although the adsorbed NO is never fully released under vacuum, it was possible to confirm the higher capacity of adsorption and release of titanoslicates [10–13,15,16]. These NO release results are not easily comparable to those described in the literature for nanoporous solids designed for the same purpose since different media, concentrations and temperature conditions were used. For instance, release studies of Zn^{2+}-exchanged zeolite carried out with a NO electrode, in 5% LB:PBS media and at 37 °C, revealed significant NO flow in the first 10 min that decreased to near zero thereafter [35]. Nevertheless, such burst efficiently inhibited bacterial growth [35]. The more sustained NO release profile obtained for ETS-4 prompted us to study its release profile at lower concentrations (Fig. 3), since at 450 μg/mL some toxicity is noticed (Fig. 1 b). These results demonstrated a time-dependent and concentration-dependent NO release over 2 h. This supports the high potential of applying this compound to achieve a control release of NO concentrations that is essential for pharmacological applications.

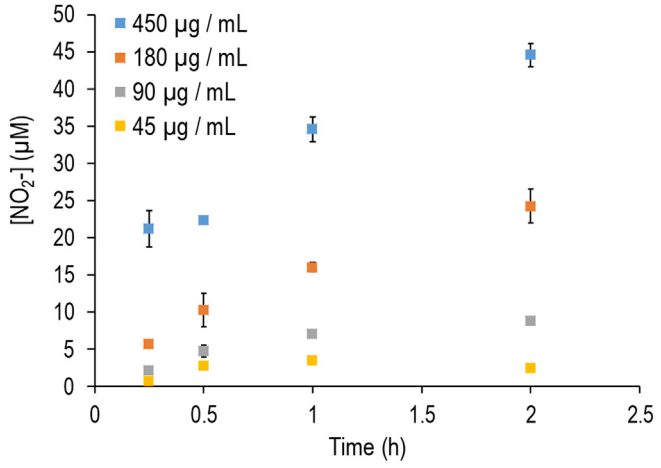

Fig. 3. Indirect nitric oxide release studies of ETS-4 at different concentrations under biological conditions.
Nitrite release levels from NO loaded ETS-4 were measured in RPMI-1640 medium at 37 °C, using Griess reagent. The error bars represent the standard deviation of eight assays.

Materials' stability is also another requirement for a successful NO carrier, being critical to ensure the storage of the gas, its controlled release and to avoid the leaching of their components in the tissues that may cause potential side reactions. Thus, the stability of the present materials under biological conditions was tested and the respective data are shown in Supplementary Table A2. Except for Cu-ETS-4 and Co-ETS-4, titanosilicates present excellent stability in HEKn cell culture by showing no release of metals to the medium, which is indicative of absence of degradation by the materials. Cu-ETS-4 and Co-ETS-4 assays, however, present a Cu^{2+} and Co^{2+} concentrations of 21.25 and 4.25 μg/mL, respectively, in the culture medium, indicating that these exchangeable cations that compensate the charge of the framework can be released/exchanged when in contact with cell culture medium. In the case of clay-based materials, all exhibit some degradation proved by considerable amounts of the correspondent metals detected in the medium.

To confirm overall results, a more comprehensive study with XRD was performed with one of those materials, namely ETS-4, by comparing its XRD pattern before and after submersion in the biological medium for 72 h (Supplementary Figure A9). The results did not present any significant changes in the material's crystallinity, which confirm its stability. Although the amount of free metals in the medium is not the only aspect that drives toxicity, overall stability results (Supplementary Table A2) are in line with the toxicity tests (Fig. 1).

3.3. Biological effects of NO-loaded materials

3.3.1. Mitochondrial respiration

To establish this new class of NO donors as a viable alternative in the control of biological functions, the impact of the active NO released on the biological systems must be addressed. Thus, effects on the mitochondrial respiration were evaluated by measuring the oxygen consumption of digitonin-permeabilized HeLa cells exposed to NO-loaded ETS-4 using a O_2 electrochemical sensor. Fig. 4 displays the variances in the O_2 consumption profiles by exposing the cells to different concentrations of NO-loaded ETS-4 (90, 180 and 450 μg/mL). Using the lower NO donor concentration (Fig. 4 a), the mitochondrial oxygen consumption was reversibly inhibited by the material, attaining an inhibition maximum of 76.7 ± 2.4% and returning to normal values after ~2 min as the NO concentration decayed. For a higher ETS-4 concentration (180 μg/mL, Fig. 4 b), the inhibition of the respiration rate was similar (73.4 ± 1.7%) but was observed for a longer period (~2.6 min). For 450 μg/mL of NO-loaded ETS-4 (Fig. 4 c), an abrupt decrease in the oxygen consumption was observed for an even longer period (~ 4 min) caused by higher release of active NO to the medium. Calculation of oxygen consumption inhibition was not possible due to interferences in the O_2 signal caused by the high amount of solid in the suspension. Overall, the main variation observed by changing the concentration was the duration of respiration inhibition that increased with the amount of NO released, highlighting the high dependence of the NO concentration in the control of the biological effect.

3.3.2. Cell migration

To evaluate the efficiency of the released NO from the new donors in wound therapy, *in vitro* models were created. Cell migration was then evaluated using Oris™ Cell Migration Assay, with the conditions optimized for this type of solid NO carriers, with HeLa cells. This cell line was used as a starting point for these tests due to its fast growth and easy maintenance, which allows the observation of results within a few days. Fig. 5a illustrates the schematic representation of the migration assay.

Cells were exposed to different concentrations of NO-loaded ETS-4. Results demonstrated that cells treated with a concentration of 90 μg/mL of NO-loaded ETS-4 migrate faster toward the central unseeded region than untreated cells (absence of material); while ETS-4 by itself

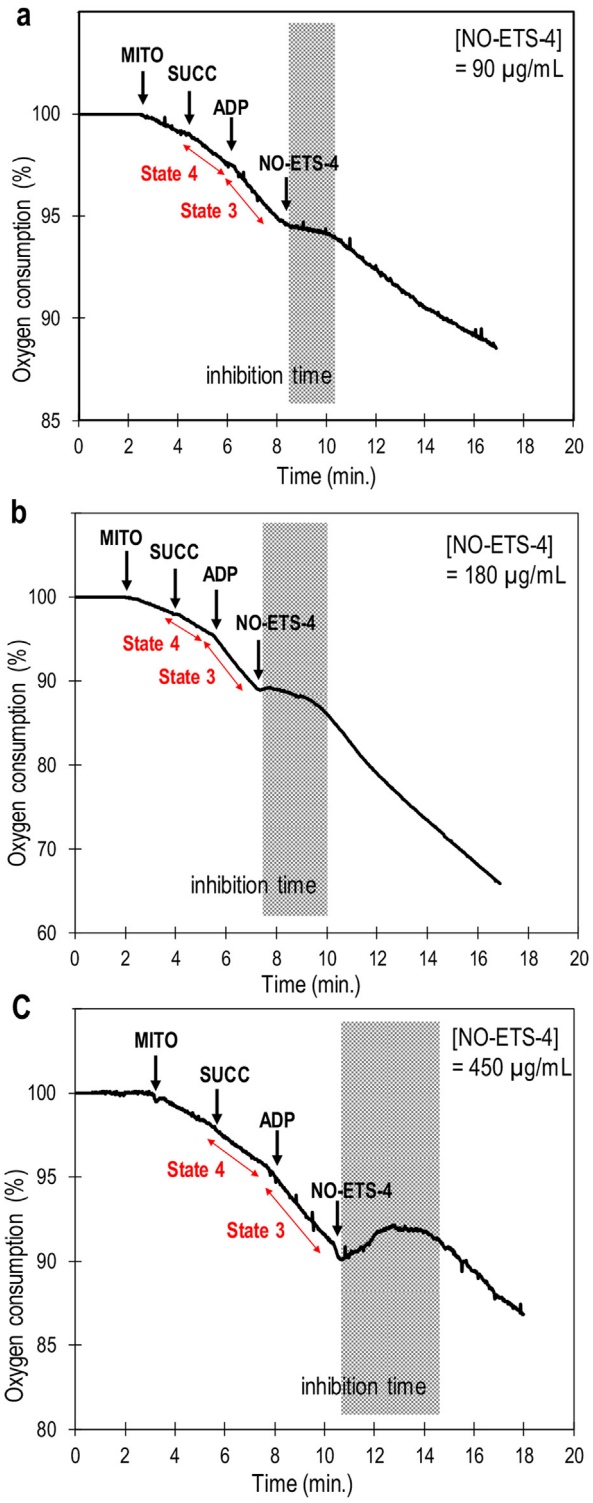

Fig. 4. Impact of NO released from ETS-4 on oxygen cell consumption. O_2 consumption profiles of digitonin-permeabilized cells (1.25 mg of protein) exposed to different concentrations of NO-loaded ETS-4: **a**) 90 µg/mL; **b**) 180 µg/mL and **c**) 450 µg/mL. The material was added after reaching the state 3 respiratory conditions, defined by the state of maximal phosphorylation after the addition of ADP.

did not show any statistically significant effect in all time points (Fig. 5 b). After 6 h of the stoppers removal (when free area starts to be accessible), cells exposed to NO donor displayed an accelerated migration and, consequently, an increased wound closure of 8±1.1% was observed, comparing with the control groups. This significant improvement remained until the end of the experiment. As revealed by comparing the microscope images (Fig. 5 c) of control cells with cells exposed to NO-loaded a ETS-4 the presence of NO greatly increased the closure of the wound after 48 h. Two other concentrations, 180 µg/mL and 45 µg/mL, of NO-loaded ETS-4 were simultaneously tested (Supplementary Fig. A10). For the lowest concentration, no differences in the migration rate were observed comparing treated cells and control, while exposing the cells to 180 µg/mL, a delay in wound closure was observed. All concentrations were ≤180 µg/mL, the same that exhibited viability above 80% after 72 h of exposure in the above described HEKn toxicity tests, thus ensuring no significant toxicity.

NO-loaded titanosilicates ETS-10 and ETAS-10 were tested at 450 µg/mL (Supplementary Fig. A11 A and B). No improvement in the wound closure was observed. Since these materials present very fast release kinetics, perhaps a higher concentration of material could enhance positive cell responses. However, this was not studied due to the concerns of the toxicological effects of the materials. The synthetic modified clay, CoOS, was also tested at 450 µg/mL (Supplementary Fig. A11 C). In this case, a slight reduction in the cell migration was verified both with NO loaded and unloaded CoOS treatment comparing with control cells without material. For this case, the toxicity effect of this material was evident at this concentration. Using lower concentrations of this material could reduce its toxicological effect and assure a more adequate NO dosage for this application. Yet, its instability (Supplementary Table A2) would certainly be a limitation, since this causes a fast and uncontrollable NO release that was confirmed by the fast release profile observed in Fig. 3 (almost all NO is released within the first 15 min).

Altogether, these results illustrate the importance of having a slow release of NO to increase cell migration, with fast-releasing compounds being ineffective. It is also important to control the concentration of NO, because NO shows biphasic behaviour with stimulatory effects turning into inhibitory effects in a relative narrow range of concentrations.

4. Discussion

The evaluation of storage capacity and kinetic release profile, material stability in culture medium and toxicity has demonstrated that not all porous materials that store NO can be considered for biological applications, namely if a fine control of biological functions is envisaged. ETS-4 proved to be the most promising material from those tested, since it is the only one that combines good biocompatibility at 180 µg/mL, high stability and controlled NO release, offering thus a great promise to be used in medical applications.

ETS-4 loaded with NO was capable of an active regulation of cells O_2 consumption in a reversible way by controlling the NO released amount (*i.e.* material concentration). Moreover, results obtained in Fig. 4 clearly show that increasing the amount of NO released, the time of respiration inhibition is longer.

Moreover, this new NO donor promoted cell migration and these encouraging results (Fig. 5) clearly highlight the potential application of this material for wound healing. Obviously, the results presented are still far from a clinical demonstration, since they were obtained with an immortalized cell type and with a stagnant media. Nevertheless, this simpler system allows us to get a first assessment of the potentiality of this new NO donor. Additionally, as showed before, sustained NO release was not maintained for 48 h since ETS-4 is unable to do so and during this time the observed effects can also arise partially from other formed species besides the NO released. Thus, applying multiple doses of NO donor over a certain period may be an option to maintain the optimal therapeutic concentration over time and obtain better results. Nevertheless, NO-based therapy for wounds treatment is challenging due to the high dependence on the specific NO concentration in the affected area: although down-regulation of NO production leads to delayed wound healing by decreasing accumulation of collagen and

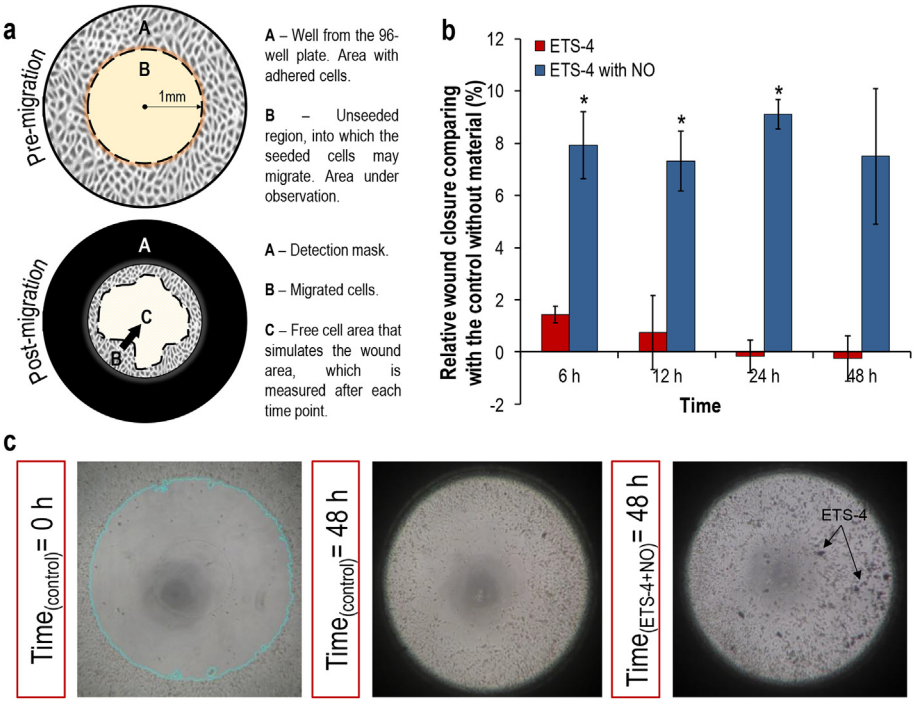

Fig. 5. Enhancement of cell migration and proliferation during Oris™ cell migration assay with NO-loaded ETS-4 using HeLa cells.
a) Scheme showing Oris™ cell migration assay in the pre-migration stage (upper figure) and post-migration stage (below figure). At given points in time, images of each condition (n = 5) were captured and free cell area was measured using software analysis. **b**) Cell migration data obtained for cells treated with NO-loaded ETS-4 and unloaded ETS-4 with a concentration of 90 μg/mL. The migration data of the control without any material represents 0% and the percentage of wound closure shown for NO-loaded ETS-4 and unloaded ETS-4 is relative to that value, i.e., the graph only shows the percentage of migration variation between untreated and treated cells. Data are reported as averages ± standard errors of the averages from three independent assays. Unpaired student's t-test was used to assess significance with p-values < 0.05 considered statistically significant (*p < 0.05). **c**) Illustrative microscope pictures captured during cell migration assay. The first image on the left, captured without a detection mask, illustrates the cells (control) in the pre-migration period (t = 0 h). The middle picture, captured with a detection mask (black area), shows the migration of the control cells after migration time (t = 48 h). The first picture from the right, captured with a detection mask, represents the post-migration cells (t = 48 h) with the NO-loaded ETS-4 (90 μg/mL), where ETS-4 particles can be noticed.

reducing wound mechanical strength [36,37], overexpression of iNOS, (i.e. excess of NO available in the wound site), may enhance the inflammatory phase of wound healing, leading to keloid lesions [38,39]. According to the literature, similar migration tests performed with huESCs cells treated with different concentrations of SNAP (a conventional donor) also confirmed the high dependence of the NO concentration in achieving positive migration responses, demonstrating that depending on the SNAP concentration, treated cells present distinct speed in the migration [40]. Therefore, NO amounts released from ETS-4 at 180 μg/mL and 45 μg/mL are not adequate for this specific application (Supplementary Figure A10). The same happened with other materials (ETS-10, ETAS-10 and CoOS, Supplementary Figure A11), which failed in demonstrate capacity to promote cell migration, perhaps not only because of their inadequate NO release profile but also because of other constraints such as the instability in biological medium and toxicity. This underlines the necessity for the more comprehensive evaluation of materials developed in this work that will guide future developments of nanoporous materials for a new therapy approach, with possible application in a broad spectrum of human diseases that would benefit from exogenous NO administration.

Acknowledgements

This work was supported by Fundação para a Ciência e a Tecnologia [IF/00993/2012/CP0172/CT0013 and PTDC/MED-QUI/28721/2017]. This work was developed in the scope of the Projects UID/MULTI/00612/2019 (CQB), UID/ECI/04028/2019 (CERENA) and FCT UID/CTM/50011/2019) (CICECO), financed by Portuguese funds through the FCT/MEC and when applicable co-financed by FEDER under the PT2020 Partnership Agreement.

RVP acknowledges for the grant 16/BAD/2017 provided by Colégio de Química, University of Lisbon.

Appendix A. Supplementary data

Supplementary data to this article can be found online at https://doi.org/10.1016/j.niox.2019.05.010.

References

[1] S. Kumar, R.K. Singh, T.R. Bhardwaj, Therapeutic role of nitric oxide as emerging molecule, Biomed. Pharmacother. 85 (2017) 182–201 https://doi.org/10.1016/j.biopha.2016.11.125.
[2] M.-M. Cals-Grierson, A.D. Ormerod, Nitric oxide function in the skin, Nitric Oxide 10 (2004) 179–193 https://doi.org/10.1016/j.niox.2004.04.005.
[3] R.P. Mason, J.R. Cockcroft, Targeting nitric oxide with drug therapy, J. Clin. Hypertens. 8 (2006) 40–52, https://doi.org/10.1111/j.1524-6175.2006.06041.x.
[4] A. Seabra, Nitric Oxide Donors: Novel Biomedical Applications and Perspectives, Elsevier Science, 2017, https://books.google.pt/books?id=iY3fDQAAQBAJ.
[5] M.R. Miller, I.L. Megson, Recent developments in nitric oxide donor drugs, Br. J. Pharmacol. 151 (2007) 305–321, https://doi.org/10.1038/sj.bjp.0707224.
[6] S.T. Gregg, Q. Yuan, R.E. Morris, B. Xiao, Functionalised solids delivering bioactive nitric oxide gas for therapeutic applications, Mater. Today Commun. 12 (2017) 95–105 https://doi.org/10.1016/j.mtcomm.2017.07.007.
[7] P.S. Wheatley, A.R. Butler, M.S. Crane, S. Fox, B. Xiao, A.G. Rossi, I.L. Megson, R.E. Morris, NO-releasing zeolites and their antithrombotic properties, J. Am. Chem. Soc. 128 (2006) 502–509, https://doi.org/10.1021/ja0503579.
[8] A.C. McKinlay, B. Xiao, D.S. Wragg, P.S. Wheatley, I.L. Megson, R.E. Morris, Exceptional behavior over the whole adsorption-storage-delivery cycle for NO in porous metal organic frameworks, J. Am. Chem. Soc. 130 (2008) 10440–10444, https://doi.org/10.1021/ja801997r.
[9] R. V Pinto, F. Antunes, J. Pires, V. Graça, P. Brandão, M.L. Pinto, Vitamin {B3} metal-organic frameworks as potential delivery vehicles for therapeutic nitric oxide, Acta Biomater. 51 (2017) 66–74 https://doi.org/10.1016/j.actbio.2017.01.039.
[10] A.C. Fernandes, F. Antunes, J. Pires, Sepiolite based materials for storage and slow release of nitric oxide, New J. Chem. 37 (2013) 4052–4060, https://doi.org/10.1039/C3NJ00452J.
[11] M.L. Pinto, J. Rocha, J.R.B. Gomes, J. Pires, Slow release of NO by microporous titanosilicate ETS-4, J. Am. Chem. Soc. 133 (2011) 6396–6402, https://doi.org/10.1021/ja200663e.
[12] M.L. Pinto, A.C. Fernandes, J. Rocha, A. Ferreira, F. Antunes, J. Pires, Microporous titanosilicates Cu^{2+}– and Co^{2+}–ETS-4 for storage and slow release of therapeutic nitric oxide, J. Mater. Chem. B. 2 (2014) 224–230, https://doi.org/10.1039/C3TB20929F.
[13] M.L. Pinto, A.C. Fernandes, F. Antunes, J. Pires, J. Rocha, Storage and delivery of nitric oxide by microporous titanosilicate ETS-10 and Al and Ga substituted analogues, Microporous Mesoporous Mater. 229 (2016) 83–89, https://doi.org/10.1016/j.micromeso.2016.04.021.
[14] A. Fernandes, F. Antunes, M.L. Pinto, J. Pires, Clay based materials for storage and therapeutic release of nitric oxide, J. Mater. Chem. B. 1 (2013) 3287–3294, https://doi.org/10.1039/c3tb20535e.
[15] A.C. Fernandes, M.L. Pinto, F. Antunes, J. Pires, Synthetic cobalt clays for the

storage and slow release of therapeutic nitric oxide, RSC Adv. 6 (2016) 41195–41203, https://doi.org/10.1039/C6RA05794B.
[16] A.C. Fernandes, M.L. Pinto, F. Antunes, J. Pires, L-Histidine-based organoclays for the storage and release of therapeutic nitric oxide, J. Mater. Chem. B. 3 (2015) 3556–3563, https://doi.org/10.1039/C4TB01913J.
[17] P.S. Wheatley, A.R. Butler, M.S. Crane, A.G. Rossi, I.L. Megson, R.E. Morris, Zeolites for storage and delivery of nitric oxide in human physiology, in: J. Čejka, N. Žilková, P. Nachtigall (Eds.), Mol. Sieves from Basic Res. To Ind. Appl. Elsevier, 2005, pp. 2033–2040 https://doi.org/10.1016/S0167-2991(05)80570-1.
[18] M. Neidrauer, U.K. Ercan, A. Bhattacharyya, J. Samuels, J. Sedlak, R. Trikha, K.A. Barbee, M.S. Weingarten, S.G. Joshi, Antimicrobial efficacy and wound-healing property of a topical ointment containing nitric-oxide-loaded zeolites, J. Med. Microbiol. 63 (2014) 203–209, https://doi.org/10.1099/jmm.0.067322-0.
[19] C.B. Lopes, P.F. Lito, M. Otero, Z. Lin, J. Rocha, C.M. Silva, E. Pereira, A.C. Duarte, Mercury removal with titanosilicate ETS-4: batch experiments and modelling, Microporous Mesoporous Mater. 115 (2008) 98–105 https://doi.org/10.1016/j.micromeso.2007.10.055.
[20] M.W. Anderson, J. Rocha, Z. Lin, A. Philippou, I. Orion, A. Ferreira, Isomorphous substitution in the microporous titanosilicate ETS-10, Microporous Mater. 6 (1996) 195–204 https://doi.org/10.1016/0927-6513(95)00098-4.
[21] Z. Lin, J. Rocha, A. Ferreira, M.W. Anderson, Synthesis of microporous titano-alumino-silicate ETAS-10 with different framework aluminum contents, Colloids Surfaces A Physicochem. Eng. Asp. 179 (2001) 133–138 https://doi.org/10.1016/S0927-7757(00)00648-8.
[22] J. Rocha, A. Ferreira, Z. Lin, M.W. Anderson, Synthesis of microporous titanosilicate ETS-10 from TiCl3 and TiO2: a comprehensive study, Microporous Mesoporous Mater. 23 (1998) 253–263 https://doi.org/10.1016/S1387-1811(98)00120-6.
[23] N.S. Bryan, M.B. Grisham, Methods to detect nitric oxide and its metabolites in biological samples, Free Radic. Biol. Med. 43 (2007) 645–657 https://doi.org/10.1016/j.freeradbiomed.2007.04.026.
[24] V. Georget, V. Baecker, ImageJ-macros: Wound Healing Tool (n.d.), http://dev.mri.cnrs.fr/projects/imagej-macros/wiki/Wound_Healing_Tool (accessed April 1, 2017).
[25] B.D. Ratner, Chapter 3 - the biocompatibility of implant materials, in: S.F. Badylak (Ed.), Host Response to Biomater, Academic Press, Oxford, 2015, pp. 37–51 https://doi.org/10.1016/B978-0-12-800196-7.00003-7.
[26] B.D. Kevadiya, R.P. Thumbar, M.M. Rajput, S. Rajkumar, H. Brambhatt, G.V. Joshi, G.P. Dangi, H.M. Mody, P.K. Gadhia, H.C. Bajaj, Montmorillonite/poly-(ε-caprolactone) composites as versatile layered material: reservoirs for anticancer drug and controlled release property, Eur. J. Pharm. Sci. 47 (2012) 265–272, https://doi.org/10.1016/j.ejps.2012.04.009.
[27] M. Ferenc, N. Katir, K. Milowska, M. Bousmina, J.-P. Majoral, M. Bryszewska, A. El Kadib, Haemolytic activity and cellular toxicity of SBA-15-type silicas: elucidating the role of the mesostructure{,} surface functionality and linker length, J. Mater. Chem. B. 3 (2015) 2714–2724, https://doi.org/10.1039/C4TB01901F.
[28] L.C.J. Thomassen, D. Napierska, D. Dinsdale, N. Lievens, J. Jammaer, D. Lison, C.E.A. Kirschhock, P.H. Hoet, J.A. Martens, Investigation of the cytotoxicity of nanozeolites A and Y, Nanotoxicology 6 (2012) 472–485, https://doi.org/10.3109/17435390.2011.587901.
[29] S. Laurent, E.-P. Ng, C. Thirifays, L. Lakiss, G.-M. Goupil, S. Mintova, C. Burtea, E. Oveisi, C. Hebert, M. de Vries, M.M. Motazacker, F. Rezaee, M. Mahmoudi, Corona protein composition and cytotoxicity evaluation of ultra-small zeolites synthesized from template free precursor suspensions, Toxicol. Res. 2 (2013) 270–279, https://doi.org/10.1039/C3TX50023C.
[30] R. Amorim, N. Vilaça, O. Martinho, R.M. Reis, M. Sardo, J. Rocha, A.M. Fonseca, F. Baltazar, I.C. Neves, Zeolite structures loading with an anticancer compound as drug delivery systems, J. Phys. Chem. C 116 (2012) 25642–25650, https://doi.org/10.1021/jp3093868.
[31] A.W. Carpenter, M.H. Schoenfisch, Nitric oxide release: Part II. Therapeutic applications, Chem. Soc. Rev. 41 (2012) 3742–3752, https://doi.org/10.1039/C2CS15273H.
[32] M. Feelisch, D. Kubitzek, J. Werringloer, The oxyhemoglobin assay, Methods Nitric Oxide Res. (1996) 455–478.
[33] P.N. Coneski, M.H. Schoenfisch, Nitric oxide release: Part III. Measurement and reporting, Chem. Soc. Rev. 41 (2012) 3753–3758, https://doi.org/10.1039/C2CS15271A.
[34] Y.-N. Zhao, X. Xu, N. Wen, R. Song, Q. Meng, Y. Guan, S. Cheng, D. Cao, Y. Dong, J. Qie, K. Liu, Y. Zhang, A drug carrier for sustained zero-order release of peptide therapeutics, Sci. Rep. 7 (2017) 5524, https://doi.org/10.1038/s41598-017-05898-6.
[35] S. Fox, T.S. Wilkinson, P.S. Wheatley, B. Xiao, R.E. Morris, A. Sutherland, A.J. Simpson, P.G. Barlow, A.R. Butler, I.L. Megson, A.G. Rossi, NO-loaded Zn^{2+}-exchanged zeolite materials: a potential bifunctional anti-bacterial strategy. Acta Biomater. 6 (2010) 1515–1521, https://doi.org/10.1016/j.actbio.2009.10.038.
[36] M.R. Schäffer, U. Tantry, S.S. Gross, H.L. Wasserkrug, A. Barbul, Nitric oxide regulates wound healing, J. Surg. Res. 63 (1996) 237–240 https://doi.org/10.1006/jsre.1996.0254.
[37] M.R. Schäffer, U. Tantry, F.J. Thornton, A. Barbul, Inhibition of nitric oxide synthesis in wounds: pharmacology and effect on accumulation of collagen in wounds in mice, Eur. J. Surg. 165 (1999) 262–267, https://doi.org/10.1080/110241599750007153.
[38] Y.-C. Hsu, M. Hsiao, L.-F. Wang, Y.W. Chien, W.-R. Lee, Nitric oxide produced by iNOS is associated with collagen synthesis in keloid scar formation, Nitric Oxide 14 (2006) 327–334 https://doi.org/10.1016/j.niox.2006.01.006.
[39] C.A. Cobbold, J.A. Sherratt, Mathematical modelling of nitric oxide activity in wound healing can explain keloid and hypertrophic scarring, J. Theor. Biol. 204 (2000) 257–288 https://doi.org/10.1006/jtbi.2000.2012.
[40] R. Zhan, W. He, F. Wang, Z. Yao, J. Tan, R. Xu, J. Zhou, Y. Wang, H. Li, J. Wu, G. LUO, Nitric oxide promotes epidermal stem cell migration via cGMP-Rho GTPase signalling, Sci. Rep. 6 (2016) 30687, https://doi.org/10.1038/srep30687.